HHS Public Access

Author manuscript

Nat Photonics. Author manuscript; available in PMC 2015 August 01.

Published in final edited form as:

Nat Photonics. 2015 February ; 9(2): 113–119. doi:10.1038/nphoton.2014.323.

Swept confocally-aligned planar excitation (SCAPE) microscopy for high speed volumetric imaging of behaving organisms

Matthew B. Bouchard[1], **Venkatakaushik Voleti**[1], **César S. Mendes**[2], **Clay Lacefield**[3], **Wesley B. Grueber**[4], **Richard S. Mann**[2], **Randy M. Bruno**[3], and **Elizabeth M. C. Hillman**[1,*]

[1]Laboratory for Functional Optical Imaging, Departments of Biomedical Engineering and Radiology, Columbia University, New York, NY 10027

[2]Mann Lab, Department of Biochemistry and Molecular Biophysics, Columbia University, New York, NY 10032

[3]Bruno Lab, Department of Neuroscience, Columbia University, New York, NY 10032

[4]Department of Physiology and Cellular Biophysics, Department of Neuroscience, College of Physicians and Surgeons, Columbia University Medical Center, New York, NY 10032

Abstract

We report a new 3D microscopy technique that allows volumetric imaging of living samples at ultra-high speeds: Swept, confocally-aligned planar excitation (SCAPE) microscopy. While confocal and two-photon microscopy have revolutionized biomedical research, current implementations are costly, complex and limited in their ability to image 3D volumes at high speeds. Light-sheet microscopy techniques using two-objective, orthogonal illumination and detection require a highly constrained sample geometry, and either physical sample translation or complex synchronization of illumination and detection planes. In contrast, SCAPE microscopy acquires images using an angled, swept light-sheet in a single-objective, en-face geometry. Unique confocal descanning and image rotation optics map this moving plane onto a stationary high-speed camera, permitting completely translationless 3D imaging of intact samples at rates exceeding 20 volumes per second. We demonstrate SCAPE microscopy by imaging spontaneous neuronal firing in the intact brain of awake behaving mice, as well as freely moving transgenic *Drosophila* larvae.

*corresponding eh2245@columbia.edu.

Author Contribution statement

MBB and EMCH conceived of this technique, MBB, EMCH and VV generated ray-tracing models, built the system, acquired and processed data, and prepared the manuscript. CSM, RSM and WBG provided and assisted *Drosophila* samples and CL and RMB provided and assisted with mouse models. RSM, CSM, WBG, CL and RMB all advised on image interpretation and manuscript preparation.

Conflict of interest

A patent related to this technique issued on December 31st 2013 (inventors Hillman and Bouchard). The authors are currently in licensing discussions.

Introduction

Transgenic techniques are providing ever-improving fluorescent reporters of dynamic in-vivo processes such as neuronal activity and motility[1,2]. As a result, there is a growing need for high-speed, 3D volumetric optical microscopy methods that can capture these events invivo. Here, we introduce swept, confocally-aligned planar excitation (SCAPE) microscopy, a single-objective, fully translationless light-sheet imaging technology that offers substantial improvements in volumetric imaging speeds over existing microscopy techniques. SCAPE acquires optically-sectioned 3D data in the geometry of a standard epi-fluorescence microscope, and requires no translation of the objective or sample, making it capable of capturing the 3D dynamics of diverse samples including the intact rodent brain and freely moving whole organisms such *Drosophila* larvae at rates exceeding 20 volumes per second.

Conventional light-sheet imaging techniques illuminate the sample from the side using a thin sheet of light, and acquire images of the illuminated plane using an orthogonally aligned second objective[3-5]. The sample is then translated relative to this co-aligned plane to form a 3D volumetric image. This dual-objective geometry, and the need for side-on illumination and physical translation are major limitations, requiring complex sample mounting and positioning that restricts the types of samples that can be imaged, and limits achievable volumetric imaging speeds. Recent advances have achieved higher speed light sheet imaging using coordinated scanning of the light sheet with translation of the detection focal plane, either via piezoelectric movement of the orthogonal detection objective[6] or an electrically tunable lens[7]. However, the maximum volumetric imaging speeds reported in these cases did not exceed 1 Hz for volumes equivalent to SCAPE, and both configurations still required restrictive dual orthogonal objectives. Other approaches have rotated the standard light-sheet geometry by 45 degrees making it easier to image un-mounted samples, yet still requiring the same dual-objective configuration as well as physical translation of the sample with respect to the objectives for volumetric imaging[8,9]. Only one other light-sheet technique has been implemented through a single objective, although volumetric imaging still required the use of piezoelectric objective scanning with a limited field of view[10]. In all cases, piezoelectric objective scanning is inherently limiting both to acquisition speeds, and the types of in-vivo samples that can be imaged.

For in-vivo rodent brain imaging, two-photon microscopy has become the method of choice to capture neuronal activity via genetically encoded calcium indicators[1,2]. However, two-photon microscopy generally requires sequential scanning of a single point to generate volumetric images, forcing trade-offs between 3D imaging speed, resolution and field of view[11-14]. Wide-field, multi-spot and temporal focusing implementations can improve parallelization but add significant cost and complexity and still require piezoelectric objective scanning[15]. Random access scanning using acousto-optic deflectors, which visits a subset of locations within the sample to increase speed, is currently the favored approach for rapidly recording the activity of multiple neurons in the intact brain[16]. However, this approach is highly sensitive to motion, requires a-priori selection of specific neuronal cell bodies and would be very challenging to implement in freely moving organisms[17,18].

SCAPE overcomes many of the limitations described above, combining optical sectioning via oblique light-sheet illumination with a unique scanning-descanning configuration that permits high speed, translationless volumetric imaging of diverse, unmounted samples through a single, stationary objective lens. We demonstrate the ability of SCAPE to image both the superficial layers of the awake behaving mouse brain and in freely moving *Drosophila melanogaster* larvae. These samples are inaccessible to conventional light-sheet imaging approaches, and while our single-photon implementation of SCAPE cannot compete with the penetration depth of two-photon microscopy, our demonstrated volumetric imaging speeds far exceed those achievable with standard laser scanning microscopy.

The imaging geometry of SCAPE is shown in Figure 1a-b. The sample is illuminated by an oblique sheet of laser light emerging from the edge of the objective lens, exciting fluorescence within a thin, diagonal plane. A slow-moving scanner (here a polygon mirror mounted on a galvanometer motor), changes the angle of the light entering the back of the objective lens, which causes the illumination plane to sweep within the sample. Light emitted from the illuminated plane is collected by the same objective lens, and could simply be focused to form an oblique, moving image of the illuminated plane. However, reflecting the emission light off an adjacent facet of the scan mirror de-scans the light in the same way as confocal theta microscopy[19], forming a stationary ‘oblique image plane’ that is always co-aligned with the moving light sheet (see modeling in Supplemental Figure S2). Image rotation optics can then be used to project this oblique image plane onto the face of a high speed 2D camera[20] (see Supplemental Figure S1 and supplemental methods for full optical layout). SCAPE thus acquires 3D volumes by capturing high speed images as the light-sheet is swept back and forth through the sample, with each camera frame being equivalent to one y’-z’ oblique section for each light sheet location (x’), as illustrated in Figure 1c. No translation of the sample or objective lens is required, and one full 3D volume is acquired within a single < +/−4° sweep of the scan mirror.

This unusual geometry provides a slightly non-Cartesian field of view, as illustrated in Figure 1b. Figure 1d illustrates the factors governing SCAPE resolution, while Figure 1e provides an example of a simulated SCAPE point spread function (PSF). Supplemental section S1 provides further demonstration that the theoretical diffraction-limited lateral (x-y) and axial (z) resolutions of the SCAPE imaging geometry rival conventional light sheet microscopy at 0.4-2 microns and 1-3 microns respectively over large fields of view. A 600 × 1000 × 550 micron x-y-z field of view is demonstrated for our current system in non-scattering phantom measurements in Supplemental Section S2, where the limiting effects of light scattering on penetration depth and resolution are also characterized in tissue-mimicking phantoms and the in-vivo mouse brain.

In terms of imaging speed, since SCAPE requires no movement beyond sweeping the scan mirror back and forth at the ~10-40 Hz volume rate, imaging speed is limited primarily by camera frame-rate (and signal to noise). The volume rate is equal to the camera's framerate divided by the number of angular sampling steps desired in the volume. Our current Andor Zyla sCMOS camera can be binned to read-out 2560 × 80 (lateral (y’) × depth (z’)) images at 2,404 fps, such that a volume with 50, 100 and 200 ‘scan angles’ (x’) would be imaged at 48, 24 and 12 volumes per second (VPS) respectively. Commercially available cameras

could feasibly acquire data at rates exceeding 300 VPS, as detailed in supplemental section S3. The large lateral width of our sCMOS camera chip enabled insertion of a spectral image-splitter permitting exactly simultaneous dual-color imaging with side-by-side fields of view up to 1280 voxels wide, with no effect on imaging speed.

For conventional laser scanning microscopy, assuming a 1 MHz pixel rate and no overhead for physical z-scanning, an equivalent 100 × 1280 × 80 (x,y,z) voxel volume could be acquired at 0.1 VPS (one volume per 10 seconds, or 240 times slower than the 24 VPS rate of our current SCAPE system). Even at the Ti:Sapphire repetition rate of 80 MHz (the fundamental pixel-rate limit for two-photon microscopy) the maximum equivalent volume rate would be 7.8 VPS.

Here, we demonstrate the performance of SCAPE microscopy in two challenging in-vivo systems of relevance to current neuroscience and biomedical research: We demonstrate that SCAPE microscopy (using single-photon 488 nm illumination) can image spontaneous GCaMP transients in dendritic branches in cortical layers I/II in awake behaving mice with sufficient spatiotemporal resolution to resolve different onset and decay dynamics at different depths within a single 3D dendritic branch. Our *Drosophila* imaging examples address the recent trend in neuroscience towards imaging small organisms, where the whole body, brain and nervous system can feasibly be imaged in their entirety[6,21], extending previous results by capturing dynamic cellular function during spontaneous motion and behavior. We demonstrate volumetric imaging of peristaltic crawling, the beating heart, neuronal tracking and both the motion and calcium dynamics of muscle contraction within freely moving larvae at 20 VPS.

Results

All data shown were acquired using an Olympus XLUMPlanFl 20x/0.95W or 20x/1.0W objective in an upright epifluorescence geometry and a 30 mW, CW 488 nm laser with between 0.5 and 5 mW incident at the sample. All data shown are in the SCAPE ‘raw’ coordinate system (lateral (y’) × scan angle (‘x) × oblique depth (z’), see Figure 1b), with fields of view determined via post-experiment system calibrations (see Supplemental Methods).

In-vivo rodent brain imaging

Figure 2 shows SCAPE imaging of in-vivo mouse brain. Figure 2c shows a SCAPE volume rendering, while Figure 2d shows a range of x’-y’ depth-slices acquired in a head-fixed, awake behaving mouse expressing GCaMP6f in layer V pyramidal neurons of the whisker barrel cortex, with intravascular Texas red dextran labeling blood vessels. Images were acquired at 488 nm excitation with a dual-color image splitter in place. The dual-color 350 × 800 × 105 micron volumes (corresponding to 100 × 500 × 80 voxels x’-y’-z’) were imaged at 10 VPS. Supplemental movie M1 shows this dataset in detail, including 4D dynamic sequences in which blood flow in each vessel and spontaneous neuronal firing in superficial dendrites can be seen. Figure 2e shows a comparison between in-vivo two-photon microscopy and high-resolution SCAPE in a mouse with intravascular dextran conjugated fluorescein. At a depth of 140 microns, single capillaries (5-10 microns in size) can be

resolved, while diving vessels exhibit higher contrast than in two-photon microscopy. Supplemental movie M2 shows this full image stack to a depth of 200 microns, while Supplemental Figure S7 shows that larger vessels can be resolved to depths of almost 300 microns. See methods and supplemental methods for animal preparation, alignment and imaging and parameters.

Figure 3 shows SCAPE data from a mouse expressing GCaMP5g in layer 5 pyramidal neurons. Single-color 600 × 650 × 134 micron volumes (corresponding to 240 × 200 × 40 voxels x'-y'-z') were imaged at 10 VPS (using 2×2 camera binning and no image splitter). 180 seconds of data were captured just as the head-fixed mouse was waking from isoflurane anesthesia (mouse was fully awake by the end of the scan).

Figure 3b shows a two-photon image stack acquired in the same animal for reference. Figure 3c shows SCAPE volume renderings of individual dendritic trees within layers I/II, distinguished from one another and color-coded based on their unique firing dynamics, as shown in Figure 3d[22]. The time-courses shown in Figure 3d are just 10 of many distinct neuronal firing patterns observed over the 180 second acquisition period (see Supplemental Figure S9 for more analysis). Time-courses were extracted from small regions of interest over individual dendrites, and are shown raw, without filtering or interpolation. Individual firing events can be cleanly distinguished and exhibit the classical pattern of GCaMP onsets and decays. Subtle differences in temporal shape can also be discerned, even within a single dendritic tree. Figure 3e shows volumetric maps of onset and decay τ (where $F(t) = F(t_0)e^{-t/\tau}$) for a single firing event (at t = 113.5 seconds). Time-courses extracted from 2×2×1 voxel ROIs at different depths within these branches corroborate these maps, revealing that two of the dendrite's branches have similar firing dynamics, while one branch has regions with very different onset and decay transients (Figure 3f). The same behavior can be seen in the firing event in the same dendrite which occurs 8 seconds before the larger amplitude event, demonstrating that the behavior is a property of this neuron and not a transient effect. Supplemental movie M3 shows a rendering of the full 4D dynamic data set in real time.

Imaging freely moving whole organisms

Drosophila larvae of different ages and sizes, between 1st and 3rd instar, were imaged while freely moving on a glass slide in phosphate buffered saline (Figure 4a). In some cases agarose channels were used to restrict sideways motion. Figure 4 shows SCAPE images of 1st instar myosin heavy chain (mhc)-Gal4,UAS-CD8:GFP larvae in which all muscles including the body wall, the heart tube and smooth muscle in the gut are expressing green fluorescent protein (GFP)[23,24] (Supplemental Figure S10 shows two-photon images of a similar larva). A 430 × 1330 × 134 micron field of view (corresponding to 120 × 800 × 80 voxels to x'-y'-z') was imaged at 20 VPS while the animal moved freely. Figure 4b shows a SCAPE volume rendering of the whole body, while Figure 4c shows a sequence of three sequential SCAPE x'-y' image planes at two different depths, capturing the beating of the heart tube. The kymograph below (Figure 4e) shows the average of two depth planes, taken from a single lateral scan position, capturing both a peristaltic wave of circumferential muscle contraction and the rhythmic beating of the heart tube at 2-3 beats per second.

Supplemental movies M4 and M5 show multi-plane and volumetric movies of this complete dataset.

Figure 5a-b shows data from a 3rd instar mhc-Gal4, UAS-GCaMP6f, UAS-CD8:mCherry larva co-expressing mCherry and GCaMP6f in its muscles[2]. One point on the larva's ventral side was affixed to the glass side to restrict its forward motion. A dual-color, 300 × 1000 × 264 micron field of view (corresponding to 100 × 300 × 100 voxels x'-y'-z') was imaged at 10 VPS, with both fluorophores excited at 488 nm. The field of view encompasses the probing 'head' of the large larva as it reaches out and withdraws. The SCAPE image sequence shown captures complex 3D dynamics of muscle motion and contraction, in parallel with intracellular calcium dynamics revealing pulses of GCaMP fluorescence as each muscle contracts (see Supplemental movie M6). Figure 5c shows GCaMP calcium dynamics extracted from another larva whose motion was more restricted.

Figure 5c-d shows data acquired on a 1st instar NompC-QF; QUAS-tdTomato x ppk-Gal4; UAS-mCD8::GFP larva co-expressing TdTomato and GFP in two neuronal subtypes: class III dendritic arborization (da) sensory neurons + chordotonal neurons and class IV da sensory neurons respectively. Figure 5d shows volume renderings of the dual-color 260 × 800 × 265 micron field of view (corresponding to 80 × 240 × 100 voxels x'-y'-z') acquired at 10 VPS. The image sequence shows selected (non-sequential) frames that depict a wave of 3D motion of the neurons as the animal crawls forward. Autofluorescence of food in the animal's gut can also be seen[25]. A 4D motion-tracking algorithm was written in Matlab™ to track the location of individual neurons in 4D space, as shown in Figure 5e. While these neurons were not expressing GCaMP, these data demonstrate the feasibility of using SCAPE to both continuously track and measure the signal from individual neurons in freely moving whole organisms, where dual-color labeling (as in Figure 5a) could be used to ratiometrically account for motion-dependent changes in detected signal. Figure 5c shows a SCAPE volume rendering of a larva from the same strain, acquired ex-vivo at very high scanning resolution. While trade-offs in sampling rates are made to permit high-speed imaging over large volumes, this image demonstrates the very high intrinsic resolution of SCAPE, where individual cell bodies and processes can be resolved clearly.

Discussion

SCAPE is a new, high speed volumetric microscopy approach capable of imaging 3D structure and function in a diverse range of intact, living, freely moving samples. SCAPE's simple, translationless, single-objective configuration provides significant advantages over multi-objective light sheet geometries, while delivering order of magnitude improvements in volumetric imaging speeds compared to conventional laser scanning microscopy techniques. Compared to wide-field techniques such as spinning-disc confocal, SCAPE removes the need for physical z-scanning, while leveraging the benefits of selective plane illumination and thus reducing photodamage for in-vivo imaging. Our simulations and phantom measurements demonstrate that SCAPE brings these many benefits with only moderate trade-offs to resolution and penetration depth compared to conventional confocal and light-sheet microscopies.

All SCAPE images shown herein were acquired using an inexpensive benchtop prototype constructed with off-the-shelf optical components and a 30 mW 488 nm laser. All data are shown as-acquired, with no reconstruction or deconvolution[26,27]. In addition to the alternative high-NA configurations described in supplemental section S1, we anticipate that improvements to resolution and penetration depth could be achieved using red-shifted fluorophores[28], model-based or inter-plane deconvolution procedures[29] and optical components optimized for off-axis transmission. More advanced implementations of SCAPE could include using two-photon excitation (e.g. with linear swept excitation as in[30], as well as IR-shifted excitation wavelengths for improved penetration[31-33]), stimulated emission-depletion (STED), to restrict the light-sheet thickness,[34] and Bessel-beam-type or structured light implementations to improve resolution[30,35]. We note also that the en-face, translationless configuration of SCAPE makes it ideal for combination with second-beam structured light excitation techniques that could permit video-rate volumetric microscopy of the living brain with simultaneous optogenetic manipulation of cellular activity[36,37].

Our SCAPE results in the brains of awake, behaving mice demonstrated the enormous benefit of full volumetric imaging, even in superficial cortical layers. Sampling all points in the volume allowed all spontaneous activity to be captured, without requiring motion-sensitive and time-consuming a-priori selection of regions of interest, and permitting 3D volume rendering of dendritic trees based on their spontaneous dynamics. While the spatial resolution of our bench-top SCAPE prototype is certainly worse than that of two-photon microscopy in mouse brain, resolution was shown to be sufficient for complex 3D analysis of neuronal dynamics at very high sample rates. Our *Drosophila* results demonstrated SCAPE imaging of large 3D fields of view at up to 20 VPS, capturing the freely moving behavior and cellular function of 1st to 3rd instar, motile larvae. The ability to perform real-time 3D sampling of the complete brain and nervous system in an entire, awake behaving organism, at cellular resolution is a new frontier for biological and neuroscience research.

Our low-cost SCAPE prototype is compact, simple to use, and provides results in real-time. We thus envisage many additional applications of SCAPE, ranging from imaging cellular replication, function and motion in 3D cell cultures, intact and engineered tissues[38-40], to imaging 3D dynamics in microfluidics and flow-cell cytometry systems[41-43]. Endoscopic or GRIN-lens based implementations of SCAPE are feasible for invasive imaging in animals and perhaps humans. At a range of magnifications, SCAPE could also be used for applications such as dynamic surface profilometry or 3D particle velocimetry in settings beyond the life sciences.

Methods

Imaging system

The layout of our current SCAPE system is depicted in Supplemental Figure S1. The main components of the system are: 1) An Olympus XLUMPlanFl 20×/0.95W or 20×/1.0 objective lens, 2) A 30 mW, CW 488 nm laser (Melles-Griot, 85-BCD-030-115) providing between 0.5 and 5 mW incident at the sample. 3) The system's scanning element, a light-weight 12-sided polygonal scanning mirror (Lincoln Laser, DT-12-138-043) custom-mounted on a galvanometer motor (6240HA, Cambridge Technology). 4) A Photometrics

DV-2 image splitter for dual color imaging and 4) An Andor Zyla sCMOS camera (Zyla-5.5-CL10). All other parts are standard optical components. The full configuration of our prototype, as well as calibration procedures are described in supplemental methods.

Live mouse imaging

The mice shown in Figure 2a-d and Figure 3 were transgenic mice expressing Cre recombinase in cortical Layer V pyramidal neurons (Rbp4:Cre, GENSAT), which received cortical injection of adeno-associated virus carrying a Cre-inducible genetically encoded calcium indicator, GCaMP (AAV2:hSyn:FLEX:GCaMP5g or 6f PENN Vector Core). Cortical injections of virus were performed in 6-8 week old male transgenic mice (~25g). The barrel cortex of each mouse was first mapped using intrinsic optical signal imaging during single-whisker stimulation in order to target the virus injection to a functionally identified region. Following injection, mice were chronically implanted with a headplate for head fixation. After recovery from surgery, animals were habituated to head fixation for two weeks before being implanted with a 2mm cranial window, under isoflurane anesthesia, and allowed to recover overnight. The following days animals were trained on behavioral tasks, and the mouse shown in Figure 3 underwent two-photon microscopy imaging during several 30-60 min behavioral sessions, performing a whisker based detection task.

During SCAPE imaging, these mice were positioned in their usual behavioral set-up under the SCAPE objective and data were acquired for sessions lasting up to 30 minutes. The mouse shown in Figure 2a-d was briefly anesthetized with isoflurane prior to SCAPE image acquisition to permit tail vein injection of ~0.1 ml of 140 μM of Texas red dextran (70,000 MW), co-labelling the vasculature in red. The animal was then head-fixed and allowed to acclimate. The mouse shown in Figure 3 was briefly anesthetized with isoflurane during head fixation. The mouse was fully awake by the end of the 180 second SCAPE scan shown.

The vascular imaging data in Figure 2e was acquired in a urethane-anesthetized wild-type mouse with an acute cranial window, and following tail vein injection of 0.1 ml of 5% Fluorescein isothiocyanate–dextran (70,000 MW, 46945-F Sigma). Following SCAPE imaging the mouse was transferred to the stage of our custom-built upright two-photon microscope[44] for comparative imaging (see supplemental methods). The mouse was positioned on a homeothermic heat pad and monitored with pulse oximetry throughout surgery and imaging.

Drosophila larvae

Live 1st – 3rd instar larvae were bred under standard conditions and selected by visual inspection under a standard Olympus BX51 epifluorescence microscope. Each larva was then washed in phosphate buffered saline (PBS) to remove surface debris, and placed in a drop of PBS on top of a glass slide. ~1mm thick spacers were used to loosely support a glass coverslip over the sample such that the upright SCAPE objective could be immersed in a drop of water on top of the coverslip without disturbing the sample. In some cases, the larva was positioned within an agarose channel, to restrict its motion during imaging. In some cases, the sample was manually translated during imaging to keep it within the field of view (e.g. Figure 4, Movie M4). The large, 3rd instar larva in Figure 5a-b was affixed to the cover

glass using a tiny drop of cyanoacrylate in the center of its ventral surface leaving its ends free to move but preventing forward motion out of the field of view. Additional larvae (not shown) were imaged with SCAPE in an inverted configuration. The larva in Figure 5c was imaged post-mortem after euthanasia in 100% ethanol for 10 minutes.

SCAPE image analysis and visualization

The relatively simple visualization and analysis presented here was performed using Matlab™ and Amira™. Planar images are shown as raw data, unless otherwise noted, with no smoothing, interpolation or registration applied. 3D volume renderings were generated using volren modules in Amira 5.2.1 (Visage Imaging) using custom colormaps. All data shown is in 'SCAPE' (x'-y'-z') image space (see Figure 1b). The SCAPE data shown in figure 2e, Supplemental Figure S7 and movie M2 was corrected for the skewing effect of the oblique light sheet by shifting each depth plane laterally by a constant, linear factor. Two-photon data was digitally rotated in the x-y plane to match the orientation of the SCAPE image field of view. See Supplemental methods for additional details and spatiotemporal analysis of dendritic firing in mouse brain, and neuronal tracking in Drosophila larvae.

Supplementary Material

Refer to Web version on PubMed Central for supplementary material.

Acknowledgments

We acknowledge the contributions of Rafael Yuste, Darcy Kelly, and Martin Chalfie and their students and staff, in particular Masakazu Agetsuma, Sean Quirin and Darcy Peterka, for assistance with early sample selection and preparation as well as the Bloomington Stock Center and Mary Baylies and Barbara Noro for fly stocks. Keith Yeager, Lauren E. Grosberg, Mohammed Shaik, Mariel Kozberg, Sharon Kim, Ying Ma and Timothy J. Muldoon provided assistance with instrumentation, optical design and sample preparation. We thank Irving Herman and Thilanka Galwaduge for assistance with PSF calculations, Liam Paninski for discussion on neuronal data analysis and Richard Levenson for guidance on applications. We thank Lincoln Laser and Cambridge Technology for assistance with scanner design and fabrication. Funding was provided by: NIH (NINDS) R21NS053684, R01 NS076628 and R01NS063226, NSF CAREER 0954796, The Human Frontier Science Program and the Wallace H. Coulter Foundation (EMCH), NIH (NINDS) R01 NS069679 and the Dana Foundation (RMB), (NINDS) R01NS070644 (RSM), (NINDS) R01NS061908 (WBG), DoD MURI W911NF-12-1-0594 (Yuste). Matthew Bouchard received NSF and NDSEG graduate fellowships. Venkatakaushik Voleti was funded by an NSF IGERT Fellowship. César S. Mendes is supported by a postdoctoral fellowship from Fundação para a Ciência e a Tecnologia, Portugal.

References

1. Akerboom J, et al. Optimization of a GCaMP calcium indicator for neural activity imaging. J Neurosci. 2012; 32:13819–13840. [PubMed: 23035093]
2. Chen T-W, et al. Ultrasensitive fluorescent proteins for imaging neuronal activity. Nature. 2013; 499:295–300. [PubMed: 23868258]
3. Dodt H-U, et al. Ultramicroscopy: three-dimensional visualization of neuronal networks in the whole mouse brain. Nature Methods. 2007; 4:331–336. [PubMed: 17384643]
4. Verveer PJ, et al. High-resolution three-dimensional imaging of large specimens with light sheet-based microscopy. Nat Methods. 2007; 4:311–313. [PubMed: 17339847]
5. Keller PJ, et al. Fast, high-contrast imaging of animal development with scanned light sheet-based structured-illumination microscopy. Nat Meth. 2010; 7:637–642.
6. Ahrens MB, Orger MB, Robson DN, Li JM, Keller PJ. Whole-brain functional imaging at cellular resolution using light-sheet microscopy. Nat Meth. 2013; 10:413–420.

7. Fahrbach FO, Voigt FF, Schmid B, Helmchen F, Huisken J. Rapid 3D light-sheet microscopy with a tunable lens. Optics Express. 2013; 21:21010–21026. [PubMed: 24103973]
8. Holekamp TF, Turaga D, Holy TE. Fast Three-Dimensional Fluorescence Imaging of Activity in Neural Populations by Objective-Coupled Planar Illumination Microscopy. Neuron. 2008; 57:661–672. [PubMed: 18341987]
9. Wu Y, et al. Inverted selective plane illumination microscopy (iSPIM) enables coupled cell identity lineaging and neurodevelopmental imaging in Caenorhabditis elegans. Proceedings of the National Academy of Sciences. 2011; 108:17708–17713.
10. Kumar S, et al. High-speed 2D and 3D fluorescence microscopy of cardiac myocytes. Optics Express. 2011; 19:13839–13847. [PubMed: 21934745]
11. Gobel W, Kampa BM, Helmchen F. Imaging cellular network dynamics in three dimensions using fast 3D laser scanning. Nature Methods. 2007; 4:73–79. [PubMed: 17143280]
12. Glickfeld LL, Andermann ML, Bonin V, Reid RC. Cortico-cortical projections in mouse visual cortex are functionally target specific. Nat Neurosci. 2013; 16:219–226. [PubMed: 23292681]
13. Jia H, Varga Z, Sakmann B, Konnerth A. Linear integration of spine Ca2+ signals in layer 4 cortical neurons in vivo. Proceedings of the National Academy of Sciences. 2014; 111:9277–9282.
14. Mittmann W, et al. Two-photon calcium imaging of evoked activity from L5 somatosensory neurons in vivo. Nat Neurosci. 2011; 14:1089–1093. [PubMed: 21743473]
15. Schrodel T, Prevedel R, Aumayr K, Zimmer M, Vaziri A. Brain-wide 3D imaging of neuronal activity in Caenorhabditis elegans with sculpted light. Nat Meth. 2013; 10:1013–1020.
16. Katona G, et al. Fast two-photon in vivo imaging with three-dimensional random-access scanning in large tissue volumes. Nat Meth. 2012; 9:201–208.
17. Grewe BF, Langer D, Kasper H, Kampa BM, Helmchen F. High-speed in vivo calcium imaging reveals neuronal network activity with near-millisecond precision. Nat Meth. 2010; 7:399–405.
18. Cotton RJ, Froudarakis E, Storer P, Saggau P, Tolias AS. Three-dimensional mapping of microcircuit correlation structure. Front Neural Circuits. 2013; 7:151. [PubMed: 24133414]
19. Dwyer PJ, DiMarzio CA, Zavislan JM, Fox WJ, Rajadhyaksha M. Confocal reflectance theta line scanning microscope for imaging human skin in vivo. Opt Lett. 2006; 31:942–944. [PubMed: 16599219]
20. Dunsby C. Optically sectioned imaging by oblique plane microscopy. Opt Express. 2008; 16:20306–20316. [PubMed: 19065169]
21. Vaziri A, Shank CV. Ultrafast widefield optical sectioning microscopy by multifocal temporal focusing. Opt. Express. 2010; 18:19645–19655. [PubMed: 20940859]
22. Hillman EMC, Moore A. All-optical anatomical co-registration for molecular imaging of small animals using dynamic contrast. Nature Photonics. 2007; 1:526–530. [PubMed: 18974848]
23. Schuster CM, Davis GW, Fetter RD, Goodman CS. Genetic dissection of structural and functional components of synaptic plasticity. I. Fasciclin II controls synaptic stabilization and growth. Neuron. 1996; 17:641–654. [PubMed: 8893022]
24. Curtis NJ, Ringo JM, Dowse HB. Morphology of the pupal heart, adult heart, and associated tissues in the fruit fly, Drosophila melanogaster. Journal of Morphology. 1999; 240:225–235. [PubMed: 10367397]
25. Bouchard MB, et al. Technical considerations in longitudinal multispectral small animal molecular imaging. J Biomed Opt. 2007; 12:051601. [PubMed: 17994870]
26. Broxton M, et al. Wave optics theory and 3-D deconvolution for the light field microscope. Optics Express. 2013; 21:25418–25439. [PubMed: 24150383]
27. Quirin, S.; Jackson, J.; Peterka, DS.; Yuste, R. Simultaneous imaging of neural activity in three dimensions. Frontiers in Neural Circuits; 2014.
28. Akerboom J, et al. Genetically encoded calcium indicators for multi-color neural activity imaging and combination with optogenetics. Frontiers in Molecular Neuroscience. 2013; 6
29. Hillman EMC, Boas DA, Dale AM, Dunn AK. Laminar Optical Tomography: demonstration of millimeter-scale depth-resolved imaging in turbid media. Opt. Lett. 2004; 29:1650–1652. [PubMed: 15309848]

30. Truong TV, Supatto W, Koos DS, Choi JM, Fraser SE. Deep and fast live imaging with two-photon scanned light-sheet microscopy. Nat Meth. 2011; 8:757–760.
31. Horton NG, et al. In vivo three-photon microscopy of subcortical structures within an intact mouse brain. Nat Photon. 2013; 7:205–209.
32. Kobat D, et al. Deep tissue multiphoton microscopy using longer wavelength excitation. Opt. Express. 2009; 17:13354–13364. [PubMed: 19654740]
33. Lavagnino Z, Zanacchi FC, Ronzitti E, Diaspro A. Two-photon excitation selective plane illumination microscopy (2PE-SPIM) of highly scattering samples: characterization and application. Opt Express. 2013; 21:5998–6008. [PubMed: 23482168]
34. Friedrich M, Gan Q, Ermolayev V, Harms Gregory S. STED-SPIM: Stimulated Emission Depletion Improves Sheet Illumination Microscopy Resolution. Biophysical Journal. 2011; 100:L43–L45. [PubMed: 21504720]
35. Planchon TA, et al. Rapid three-dimensional isotropic imaging of living cells using Bessel beam plane illumination. Nat Meth. 2011; 8:417–423.
36. Lutz C, et al. Holographic photolysis of caged neurotransmitters. Nat Methods. 2008; 5:821–827. [PubMed: 19160517]
37. Golan L, Reutsky I, Farah N, Shoham S. Design and characteristics of holographic neural photo-stimulation systems. Journal of Neural Engineering. 2009; 6:066004. [PubMed: 19837999]
38. Jing D, et al. In situ intracellular calcium oscillations in osteocytes in intact mouse long bones under dynamic mechanical loading. The FASEB Journal. 2014; 28:1582–1592. [PubMed: 24347610]
39. Carlson GC, Coulter DA. In vitro functional imaging in brain slices using fast voltage-sensitive dye imaging combined with whole-cell patch recording. Nat. Protocols. 2008; 3:249–255. [PubMed: 18274527]
40. Xie W, et al. Imaging atrial arrhythmic intracellular calcium in intact heart. Journal of Molecular and Cellular Cardiology. 2013; 64:120–123. [PubMed: 24041536]
41. Sung Y, et al. Three-Dimensional Holographic Refractive-Index Measurement of Continuously Flowing Cells in a Microfluidic Channel. Physical Review Applied. 2014; 1:014002. [PubMed: 25419536]
42. Regmi R, Mohan K, Mondal PP. Light sheet based imaging flow cytometry on a microfluidic platform. Microscopy Research and Technique. 2013; 76:1101–1107. [PubMed: 24136899]
43. Baik AD, Qiu J, Hillman EMC, Dong C, Guo XE. Simultaneous tracking of 3D actin and microtubule strains in individual MLO-Y4 osteocytes under oscillatory flow. Biochemical and Biophysical Research Communications. 2013; 431:718–723. [PubMed: 23352617]
44. Radosevich, AJ., et al. BIOMED 2008 Proceedings. OSA Technical Digest; 2007. Hyperspectral in-vivo two-photon microscopy of intrinsic fluorophores..

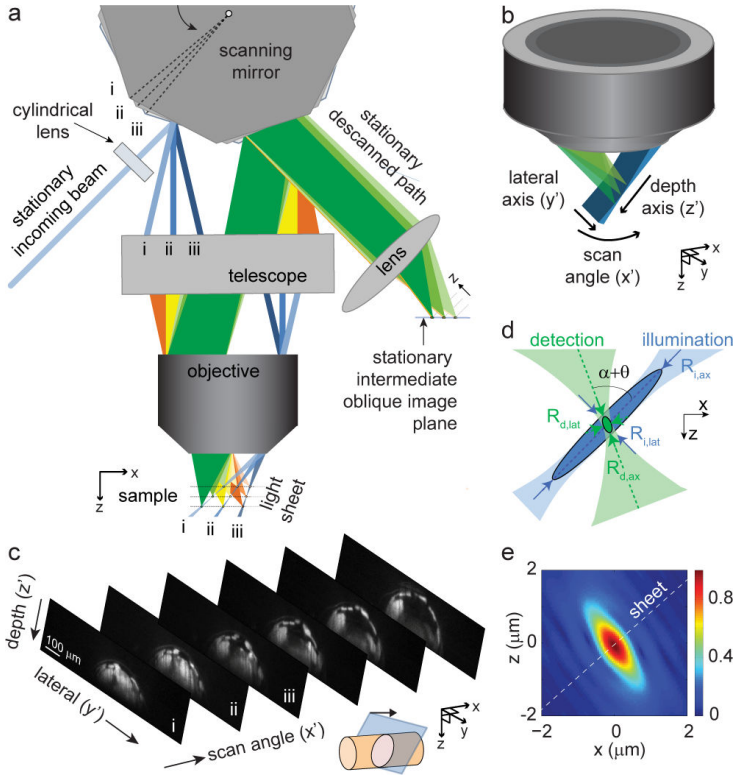

Figure 1. SCAPE imaging geometry and image formation

(a) Illustrates SCAPE's scanning-descanning geometry that sweeps an oblique light sheet back and forth across the sample while the descanned detection plane remains stationary. The only moving component is the slowly oscillating polygonal scanning mirror. (b) Shows how the oblique light sheet illuminates the sample, while emitted light is collected by the same objective lens ('scan', 'lateral' and 'depth' (x'-y'-z') directions define the non-Cartesia SCAPE coordinate system). (c) Illustrates how images are captured as the light sheet sweeps (mCherry-MHC Drosophila larva). (d) SCAPE resolution depends upon the axial and lateral resolutions of the low NA input light sheet ($Ri,_{lat}$ and $Ri,_{ax}$), the higher NA detection side ($Rd,_{lat}$ and $Rd,_{ax}$), and the relative angle between them. (e) Fourier-optics modeled point spread function (PSF) for an Olympus XLUMPlanFl 20x/0.95W objective [20, 21]. See Supplemental sections for additional optical layouts, simulations and performance analysis.

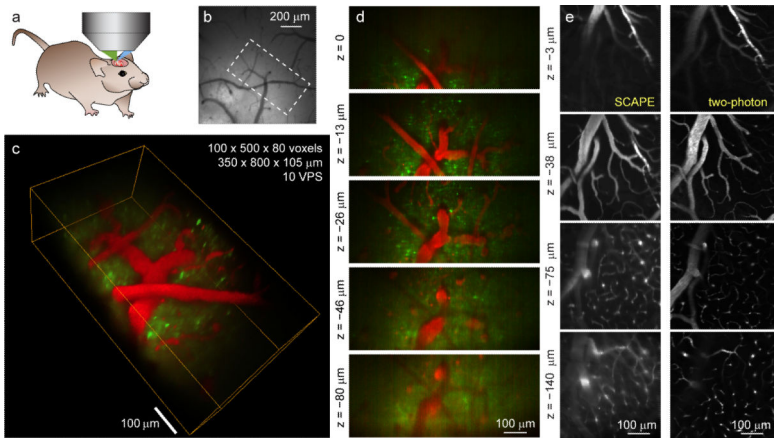

Figure 2. SCAPE microscopy in mouse brain

(a) Shows SCAPE image acquisition geometry, (b-d) Imaging in an awake, behaving mouse with intravascualar Texas red dextran (red), and GCaMP6f in superficial dendrites from layer V neurons (green). b) Camera image of exposed cortex showing approximate SCAPE field of view, c: Rendering of a single 350 × 800 × 105 microns (x'-y'-z') volume acquired in 0.1 seconds (see Supplemental movie M1). d) Individual x'-y' planes extracted from the same SCAPE volume (each plane is an average of 5 sequential time-points). (e) Comparison between two-photon microscopy and SCAPE in a urethane-anesthetized mouse with intravascular FITC-dx at 4 different depths (linear grayscale). Slower, higher x' resolution SCAPE acquisition demonstrates that 5-10 micron capillaries can be resolved to depths of at least 140 microns with 488 nm excitation. Supplemental movie M2 shows depth slices to 200 microns. Supplemental Figure S7 shows x-z and y-z projections.

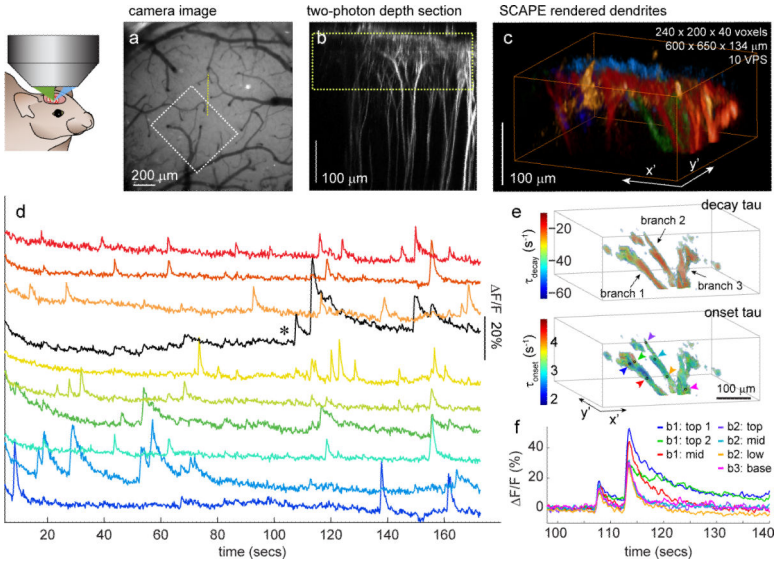

Figure 3. SCAPE microscopy of neuronal calcium dynamics in awake mouse brain

(a). Camera image of exposed cortex showing SCAPE field of view. Yellow line shows location of the conventional two-photon axial section shown in (b), yellow box indicates SCAPE depth range. (c) shows a volume rendering (Amira™ volren) of the dendritic trees captured by SCAPE, each corresponding to a specific event during the 180 second acquisition period. Color-matched raw time-courses for each dendritic tree are shown in (d) (many more events were also identified, see Supplemental Figure S7 and supplemental movie M3). (e) shows maps of onset and decay dynamics within a single dendritic tree, calculated as $F(t) = F(t0)e^{t/\tau}$. Plots in (f) show time-courses extracted from regions indicated by colored arrowheads in (e). Branches 2 and 3 (b2, b3) show very similar dynamics, while points along branch 1 (b1) exhibit very different onset and decay dynamics in both sequential firing events.

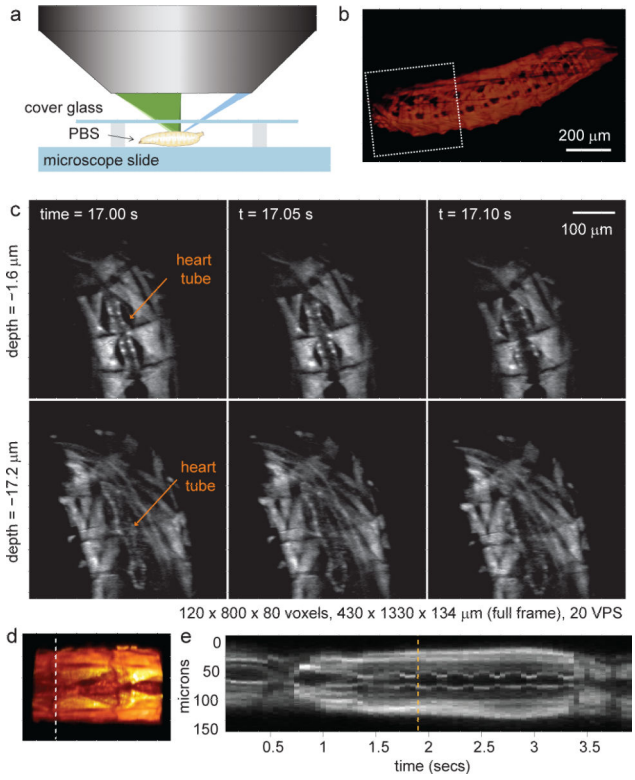

Figure 4. SCAPE of freely moving mhc-Gal4,UAS-CD8:GFP 1st instar *Drosophila* melanogaster larvae

(a) shows the en-face imaging geometry employed, in which the larva was able to freely crawl and move within the field of view. (b) Shows a large field of view SCAPE image of the entire larva. White square indicates location of zoomed images shown in (c), where different depth sections and sequential images acquired at 20 VPS reveal the dynamics of a single heartbeat (linear grayscale). (d) shows a volume rendering of a section of these data, while (e) shows a kymograph of 2 micron thick section of the y' plane indicated in (d), capturing both a peristaltic wave as the animal moves, and the rhythmic beating of its heart tube. Orange line shows the time of the volume shown in (d). Supplemental movies M4 and M5 show these data as a full 4D dynamic volume.

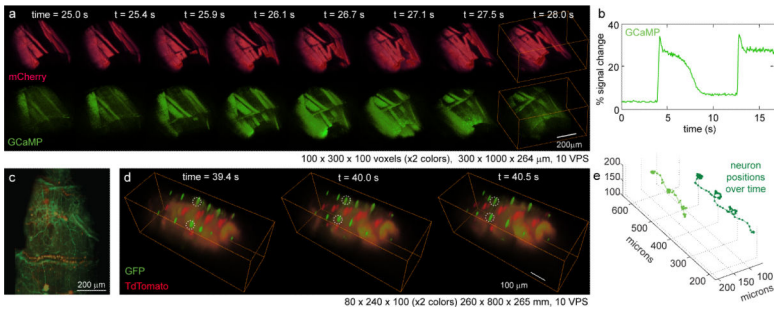

Figure 5. SCAPE microscopy of cellular structure-function and 3D cell tracking in freely moving *Drosophila* larvae

a) SCAPE volume renderings of a 3rd instar mhc-Gal4, UASGCaMP6f, UAS-CD8:mCherry *Drosophila* larva expressing both calcium sensitive GCaMP (green) and a structural mCherry (red) marker in smooth muscle. The (non-sequential) image sequence, acquired at 10 VPS, shows pulses of GCaMP6f fluorescence corresponding to muscle contractions. (b) GCaMP dynamics extracted from a slower moving larva. (c) High resolution SCAPE rendering showing sub-cellular resolution in an ex-vivo 1st instar NompC-QF, QUAS-tdTomato; ppk-Gal4, UAS-mCD8::GFP larva expressing GFP and tdTomato in class III sensory + chordotonal neurons, and class IV sensory neurons, respectively. (d) In-vivo SCAPE volume sequence (nonsequential) of same during free motion. (e) The output of a 4D motion tracking algorithm showing the 3D location of specific neurons (circles in (d)) over time, permitting extraction of dynamic intensity signals during free movement. See also supplemental movies M6-M8.